

Figure S1

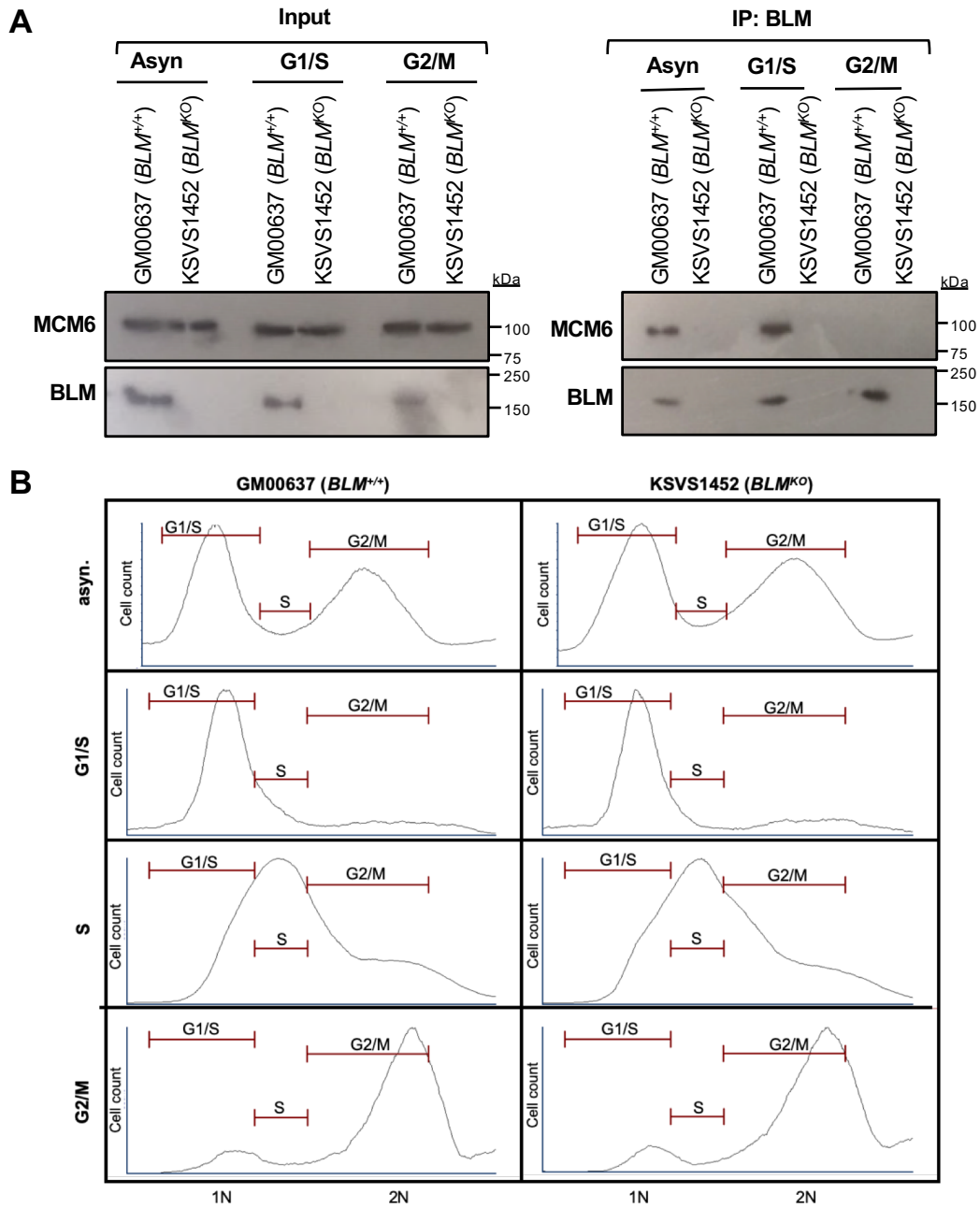


Figure S2

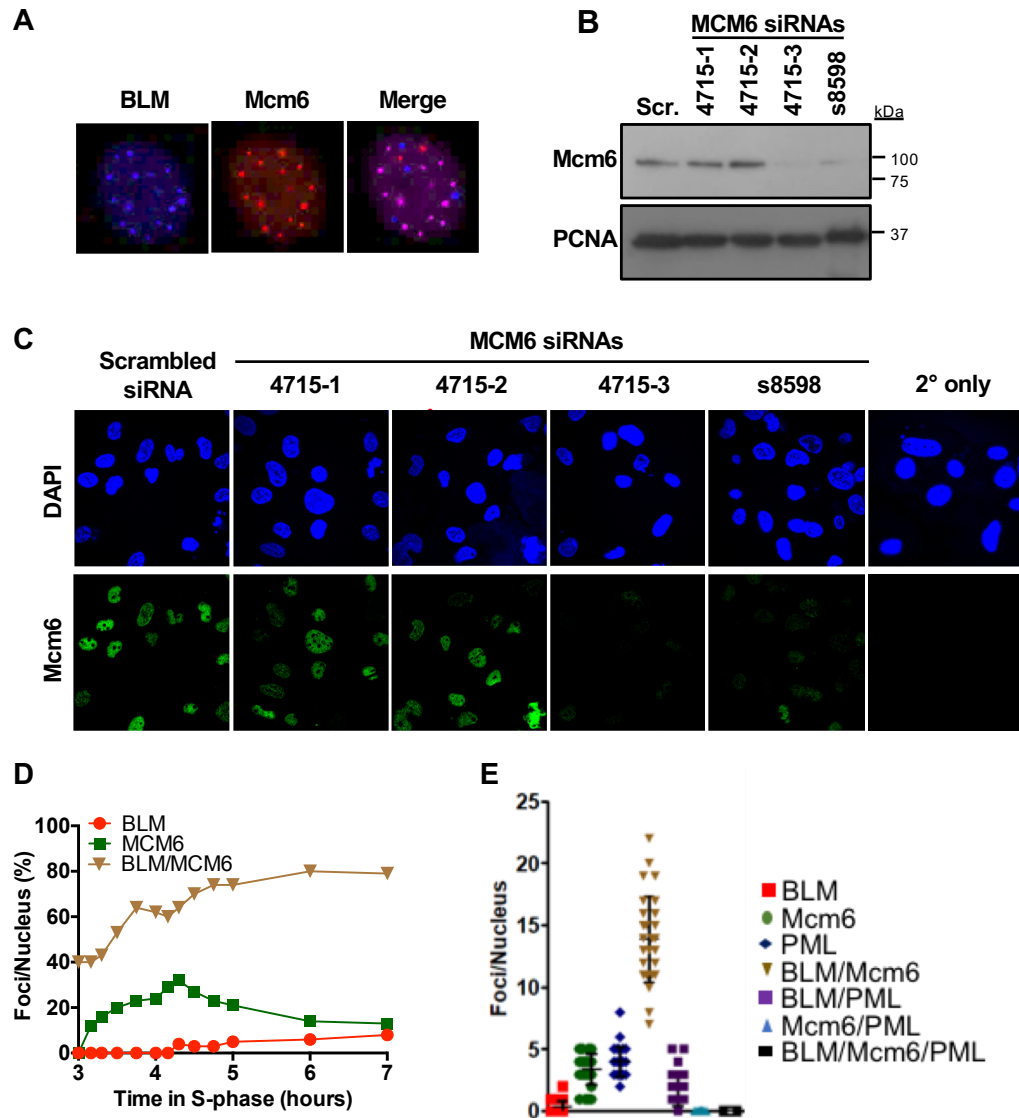


Figure S3

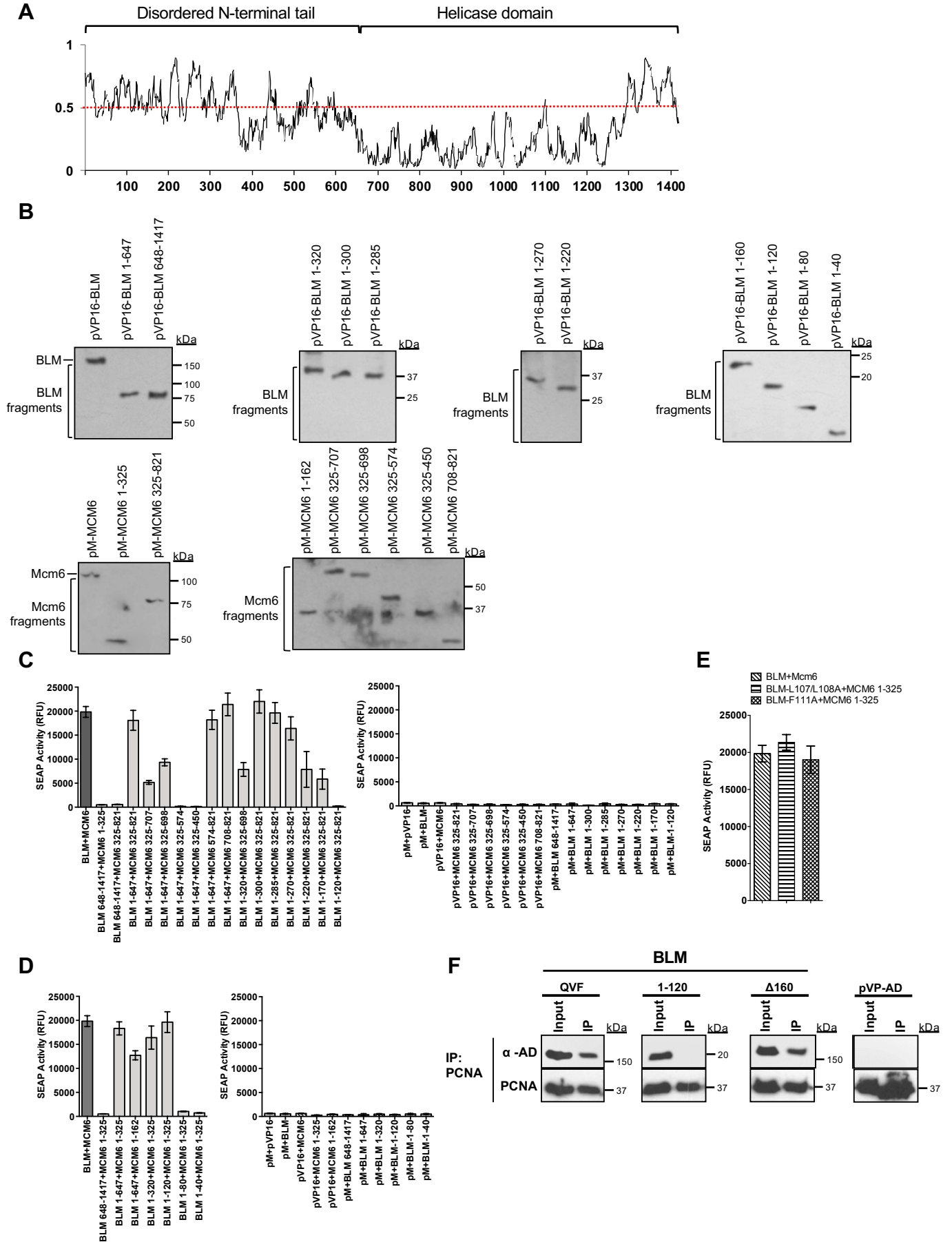


Figure S4

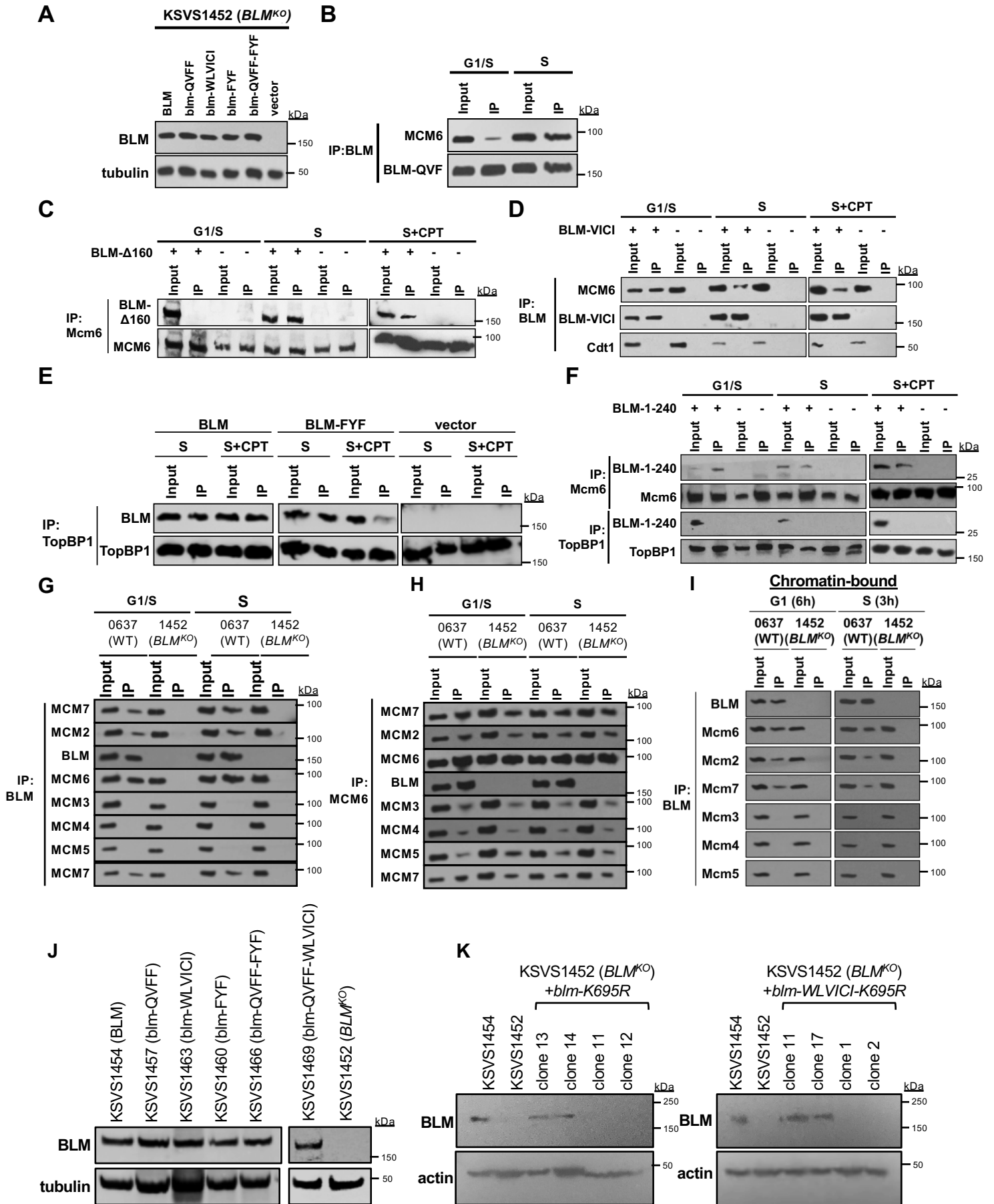


Figure S5

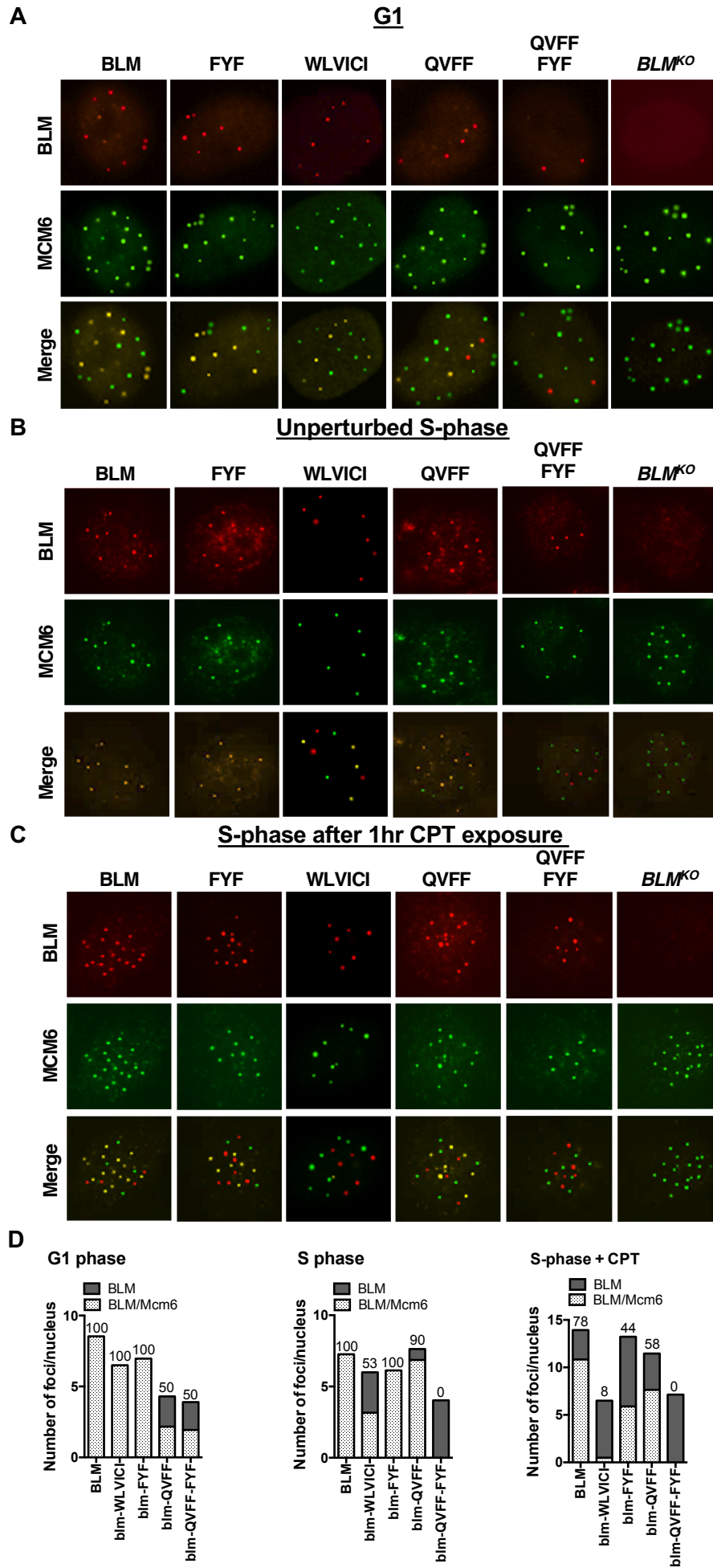


Figure S6

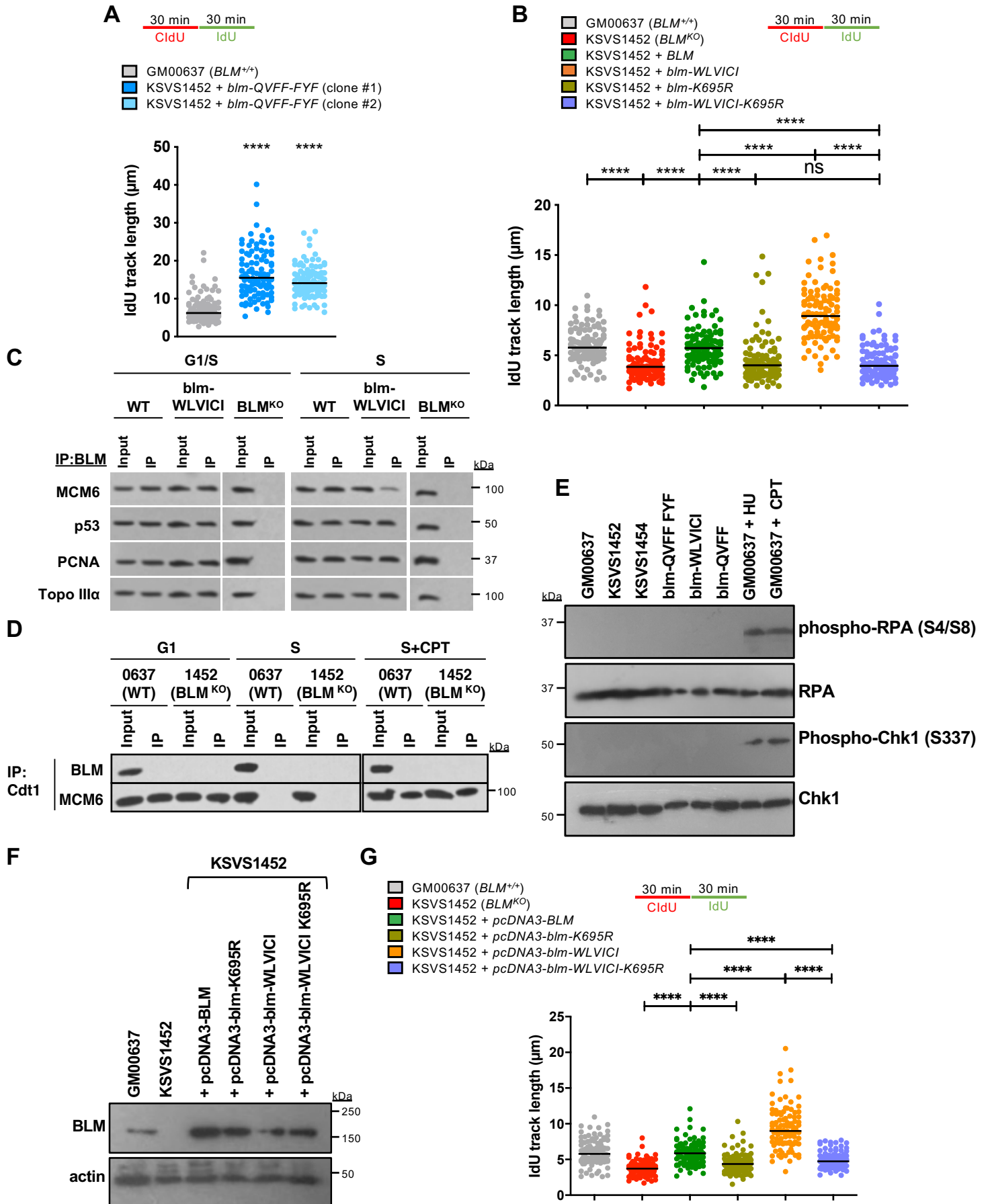
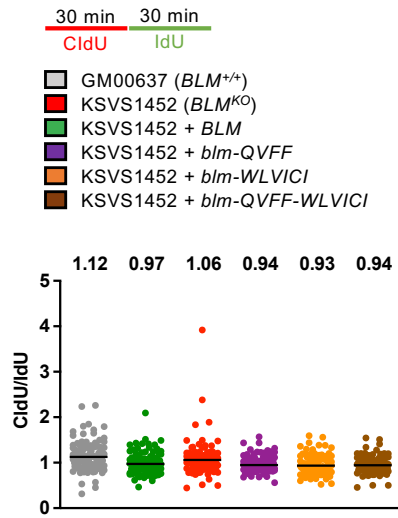
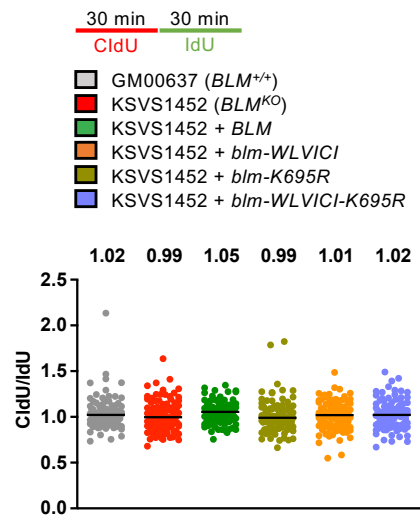


Figure S7

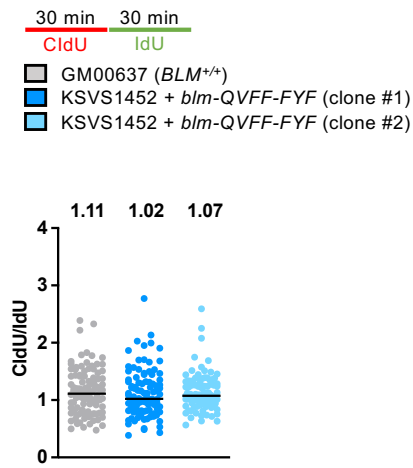
A



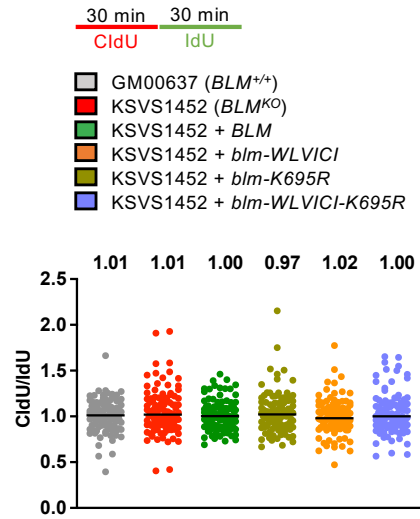
B



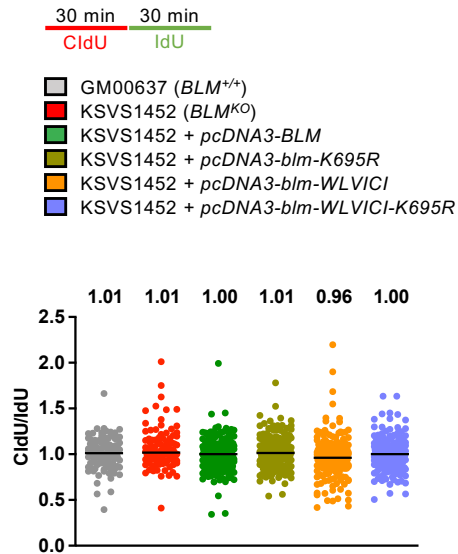
C



D



E



SUPPLEMENTAL INFORMATION

FIGURE LEGENDS

Figure S1. Absence of interaction between BLM and Mcm6 in G2/M. (A) KSVS1452 (BLM^{KO}) and GM00637 ($BLM^{+/+}$) cells were synchronized at G1/S or blocked at G2/M, and the interaction between endogenous BLM and Mcm6 assessed by co-immunoprecipitation. (B) Verification by flow cytometry of cell cycle synchronization of KSVS1452 (BLM^{KO}) and GM00637 ($BLM^{+/+}$) cells at G1/S, in S-phase (release from G1/S for 3 hours), or block at G2/M.

Figure S2. Colocalization of BLM, Mcm6 and PML in perturbed and unperturbed S-phase and expression throughout G1 phase. (A) Confocal images of GM00637 ($BLM^{+/+}$) cells showing immunostaining of endogenous BLM and Mcm6 using different antibodies than in Fig. 1E and Fig. 1F (anti-BLM [ab2179, Abcam], anti-Mcm6 [PLA0041, Sigma]). The Mcm6 antibody H-8 (SCBT) was verified by Western blotting (B) and immunofluorescence microscopy (C). Three siRNAs from Bioneer (siRNA #4715-1/2/3) and one siRNA from Life Technologies (s8598) targeting human MCM6 expression were used (50 nM) to transfect GM00637 ($BLM^{+/+}$) cells using Lipofectamine RNAiMAX (Invitrogen) in Opti-MEM medium. Cells were harvested and Mcm6 levels analyzed 48 hours after transfection. Transfection with scrambled siRNA (Silencer Select Negative Control No. 1, Invitrogen) and immunofluorescence microscopy with only secondary antibody (2°) served as controls. Scr, scrambled siRNA. (D) Quantification of BLM and Mcm6 foci per nucleus (%) and their colocalization during mid- and late S-phase in GM00637 ($BLM^{+/+}$) cells. Foci in 30 nuclei were analyzed; average percentage of foci per nucleus is reported. (E) Colocalization of BLM and Mcm6 foci with PML foci was quantified in confocal microscopy images of GM00637 ($BLM^{+/+}$) cells in the second half of S-phase (5-7 hours after release from G1/S arrest). 30 nuclei were analyzed for each of the indicated time points. Mean \pm SD is shown.

Figure S3. Identification of Mcm6 binding sites in the N-terminal tail of BLM. (A) Disorder scores for all amino acid residues of human BLM were calculated in IUPred (2). A score of >0.5 indicates a disordered residue. (B) Western blot analysis of expression of BLM and Mcm6 fragments used for two-hybrid analysis of the BLM/Mcm6 interaction. (C) Two-hybrid analysis of the interaction between the N-terminal domain of Mcm6 (residues 1-325) and fragments of BLM. Mean \pm SD from three transfections is shown. Bottom panel shows the Mcm6 and BLM fragments in combination with empty bait and prey vectors. (D) Two-hybrid analysis of the interaction between fragments of the C-terminal domain of Mcm6 (residues 325-821) and fragments of BLM. Mean \pm SD from three transfections is shown. Bottom panel shows the Mcm6 and BLM fragments in combination with empty bait and prey vectors. (E) Effect of L107A and L108A or F111A mutations in MBD-N of BLM on Mcm6 binding was analyzed by mammalian two-hybrid assay. Mean \pm SD from three transfections is shown. (F) KSVS1452 (*BLM*^{KO}) cells were transfected with plasmids pVP16 expressing the first 120 residues of BLM, or BLM lacking the first 160 residues, the blm-QVF mutant, or empty vector and interaction with endogenous PCNA was assessed by co-immunoprecipitation. BLM peptides and the blm-QVF mutant carry an AD-tag.

Figure S4. Interaction of BLM and BLM mutants with MCM and TopBP1. (A) Expression levels of BLM mutants transiently expressed from plasmid pVP16 in KSVS1452 (*BLM*^{KO}) cells were assessed by Western blot. (B) Effect of the milder blm-QVF mutation on BLM/Mcm6 interaction was determined by co-immunoprecipitation of BLM and Western blot for Mcm6. (C) Effect of deleting the first 160 residues of BLM on interaction with endogenous Mcm6 was assessed by co-immunoprecipitation. KSVS1452 (*BLM*^{KO}) cells were transfected with pVP16 expressing residues 161-1417 of BLM, synchronized at the G1/S boundary, released into S-phase for 3 hours, exposed to 1 μ M CPT for 1 hour and nuclear extracts prepared for immunoprecipitation of endogenous Mcm6. (D) Effect of the blm-VICI mutation in MBD-C on BLM interaction with endogenous Mcm6 was assessed by co-immunoprecipitation. KSVS1452 (*BLM*^{KO}) cells were transfected with pVP16 expressing the blm-VICI mutant, synchronized

at the G1/S boundary, released into S-phase for 3 hours, exposed to 1 μ M CPT for 1 hour and nuclear extracts prepared for immunoprecipitation of blm-VICI. **(E)** Co-immunoprecipitation of endogenous TopBP1 and the blm-FYF mutant transiently expressed in KSVS1452 (BLM^{KO}) cells in unperturbed S-phase and after CPT exposure. **(F)** Co-immunoprecipitation of endogenous Mcm6 and TopBP1 with the first 240 residues of BLM, which contain MBD-N and MBD-C but not MBD-D. KSVS1452 (BLM^{KO}) cells were transfected with pVP16 expressing the first 240 residues of BLM, synchronized at the G1/S boundary, released into S-phase for 3 hours, exposed to 1 μ M CPT for 1 hour and nuclear extracts prepared for immunoprecipitation of endogenous Mcm6 or TopBP1. **(G)** Co-immunoprecipitations of endogenous Mcm6 or **(H)** endogenous BLM from nuclear extracts of GM00637 ($BLM^{+/+}$) and KSVS1452 (BLM^{KO}) cells synchronized at G1/S and after release into S-phase for 3 hours. Membranes were probed for endogenous MCM proteins in the order shown, starting with Mcm7 and ending with Mcm5. At the conclusion of the hybridizations, the membrane was again probed with Mcm7 antibody to verify the integrity of protein on the membrane. **(I)** Chromatin-bound proteins were extracted from GM00637 ($BLM^{+/+}$) cells 6 hours after release from nocodazole block (G1) and 3 hours after release from G1/S block (S) and co-immunoprecipitation of BLM with Mcm6 and other MCM subunits tested. **(J)** Whole cell extracts of stable, single-cell clones were analyzed for expression of blm mutants. BLM knockout cell line KSVS1452 and KSVS1452 stably expressing wildtype BLM (KSVS1454) are shown as negative and positive controls, respectively. BLM expression was assessed using BLM antibody A300-110 (Bethyl Laboratories). **(K)** Whole cell extracts of stable, single-cell clones were analyzed for expression of the blm-K695R and blm-WLVICI-K695R mutants. Two positive clones for each BLM mutant (Supplemental Table S1) and two negative clones are shown. BLM knockout cell line KSVS1452 and KSVS1452 stably expressing wildtype BLM (KSVS1454) are shown as negative and positive controls, respectively. BLM expression was assessed using BLM antibody A300-110 (Bethyl Laboratories).

Figure S5. Effects of MBD-N, MBD-C, and MBD-D mutations on colocalization of Mcm6 and BLM

in G1, S-phase and after DNA damage. Confocal images of KSVS1452 (*BLM*^{KO}) cells expressing BLM or BLM mutants immunostained for BLM and Mcm6 in **(A)** cells in G1 obtained by 6-hour release from nocodazole block **(B)** cells in S-phase obtained by 3-hour release from the G1/S boundary, and **(C)** cells in mid-S-phase (3 hours) treated with 1 μ M CPT for 1 hour and released for 45 minutes into CPT-free media. Anti-BLM C18 (SCBT)] and anti-Mcm6-H8 (SCBT) antibodies were used. **(D)** Quantification of BLM or BLM mutant foci for colocalization with Mcm6 in 30 nuclei of cells in G1 phase, unperturbed S-phase and 45 minutes after release from 1-hour CPT exposure. Numbers above columns indicate the percentage of BLM foci that colocalized with Mcm6 foci.

Figure S6. Effect of BLM mutations on DNA replication (A) Analysis of DNA replication speed in two single-cell clones of the *blm*-QVFF-FYF mutant by DNA fiber assay. Unperturbed cells were incubated in the presence of CldU for 30 min and then in the presence of IdU for 30 min, immunostained and imaged on a Keyence fluorescence microscope. A minimum of 100 fibers showing a red region extended by a green region (elongating forks) were analyzed for each cell line. The length of the green region was used to calculate replication speed (kb min⁻¹). Median replication speed is indicated by a black horizontal line. Mann-Whitney test was performed to determine statistical significance of differences to BLM-proficient cell line GM00637: **** $p < 0.0001$. **(B)** DNA fiber analysis was used to compare replication speed between *BLM*^{KO} cells (KSVS1452) stably expressing *blm*-WLVICI, *blm*-K695R (clone #13), and a second clone of the stable *blm*-WLVICI-K695R cell line (clone #17). A minimum of 100 fibers were imaged and analyzed as in (A). Median replication speed (kb min⁻¹) is indicated above the scatter dot blot. A Mann-Whitney test was performed to determine statistical significance of differences between the cell lines expressing wildtype BLM or *blm* mutants: **** $p < 0.0001$; ns, not significant **(C)** The WLVICI mutation specifically interrupts the interaction of BLM with Mcm6 in S-phase, but not the interaction of BLM with known BLM binding proteins. Co-immunoprecipitations of BLM or the *blm*-WLVICI mutant were analyzed for the presence of Mcm6, Topo III, p53 and PCNA. **(D)** Co-immunoprecipitation of Cdt1 with Mcm6 in unperturbed GM00637

(*BLM*^{+/+}) and KSVS1452 (*BLM*^{KO}) cells and cells exposed to camptothecin. **(E)** For analysis of checkpoint activation, whole cell extracts were prepared from exponentially growing, unperturbed KSVS1452 (*BLM*^{KO}) cells stably expressing BLM or blm mutants. As positive controls, replication stress was induced in GM00637 cells (*BLM*^{+/+}) by treating with either HU (5 mM for 5 hours) or CPT (1 μ M for 24 hours). Cells were lysed in RIPA lysis buffer (supplemented with protease inhibitors and phosphatase inhibitors), cleared by centrifugation at 12 krpm for 15 min, and supernatant analyzed by Western blotting for phosphorylation of RPA and Chk1, using Phospho-RPA (Ser4/Ser8, Bethyl Laboratories) and Phospho-Chk1 (Ser 317, Cell Signaling) antibodies, respectively. **(F)** KSVS1452 (*BLM*^{KO}) were transiently transfected with pcDNA3 plasmids expressing K695R, WLVI^{CI}, and WLVI^{CI}-K695R mutants of BLM. Expression was confirmed by Western blotting of whole cell extracts and probing with BLM antibody A300-110 (Bethyl Laboratories). **(G)** DNA fiber analysis was used to compare replication speed between *BLM*^{KO} cells (KSVS1452) transiently transfected with pcDNA3 plasmids expressing BLM or blm mutants. A minimum of 200 DNA fibers were imaged and analyzed as in (B). A Mann-Whitney test was performed to determine statistical significance of differences between the cells expressing the various alleles of BLM (**** $p < 0.0001$).

Figure S7. CldU/IdU ratios of DNA fiber analyses. Ratios were calculated between the length of the first labeling pulse (CldU) and the second labeling pulse (IdU). Unperturbed cells were incubated in the presence of CldU for 30 min and then in the presence of IdU for 30 min, immunostained and imaged on a Keyence fluorescence microscope. A minimum of 100 fibers showing a red region extended by a green region (elongating forks) were analyzed for each cell line. The ratios between the length of the red (CldU) and green region (IdU) were calculated. Median ratios are indicated by a black horizontal line. A median ratio of 1 is indicative of equal DNA replication speed during the two labeling periods. **(A)** CldU/IdU ratio for IdU track lengths shown in Figure 5A, **(B)** CldU/IdU ratio for IdU track lengths shown in Figure 5B, **(C)** CldU/IdU ratio for IdU track lengths shown in Supplemental Figure S6A, **(D)** CldU/IdU

ratio for IdU track lengths shown in Supplemental Figure S6B, and **(E)** CldU/IdU ratio for IdU track lengths shown in Supplemental Figure S6G.

REFERENCES

1. Shastri, V.M. and Schmidt, K.H. (2016) Cellular defects caused by hypomorphic variants of the Bloom syndrome helicase gene BLM. *Molecular genetics & genomic medicine*, **4**, 106-119.
2. Dosztanyi, Z., Csizmok, V., Tompa, P. and Simon, I. (2005) The pairwise energy content estimated from amino acid composition discriminates between folded and intrinsically unstructured proteins. *J Mol Biol*, **347**, 827-839.

Table S1. Cell lines constructed for this study

Cell line ID	Parental cell line	Relevant <i>BLM</i> genotype	Reference
KSVS1452	GM00637 ¹	<i>BLM</i> c.del2040_2046/ <i>BLM</i> c.delins2036_2041AG	30
KSVS1454	KSVS1452	<i>BLM</i>	30
KSVS1455	KSVS1452	<i>BLM</i>	30
KSVS1456	KSVS1452	<i>BLM</i>	30
KSVS1457	KSVS1452	<i>blm</i> -QVFF	This study
KSVS1458	KSVS1452	<i>blm</i> -QVFF	This study
KSVS1459	KSVS1452	<i>blm</i> -QVFF	This study
KSVS1460	KSVS1452	<i>blm</i> -FYF	This study
KSVS1461	KSVS1452	<i>blm</i> -FYF	This study
KSVS1462	KSVS1452	<i>blm</i> -FYF	This study
KSVS1463	KSVS1452	<i>blm</i> -WLVICI	This study
KSVS1464	KSVS1452	<i>blm</i> -WLVICI	This study
KSVS1465	KSVS1452	<i>blm</i> -WLVICI	This study
KSVS1466	KSVS1452	<i>blm</i> -QVFF-FYF	This study
KSVS1467	KSVS1452	<i>blm</i> -QVFF-FYF	This study
KSVS1468	KSVS1452	<i>blm</i> -QVFF-FYF	This study
KSVS1469	KSVS1452	<i>blm</i> -QVFF-WLVICI	This study
KSVS1470	KSVS1452	<i>blm</i> -QVFF-WLVICI	This study
KSVS1471	KSVS1452	<i>blm</i> -QVFF-WLVICI	This study
KSVES1501	KSVS1452	<i>blm</i> -K695R (clone 13)	This study
KSVES1502	KSVS1452	<i>blm</i> -K695R (clone 14)	This study
KSVES1503	KSVS1452	<i>blm</i> -WLVICI-K695R (clone 11)	This study
KSVES1504	KSVS1452	<i>blm</i> -WLVICI-K695R (clone 17)	This study

¹ GM00637 was obtained from the NIGMS Human Genetic Cell Repository at the Coriell Institute.